The Higgs Portal from LHC to ILC

Christoph Englert

Institute for Particle Physics Phenomenology, Department of Physics, Durham University, United Kingdom

DOI: will be assigned

Interpretations of searches for the Higgs boson are governed by model-dependent combinations of Higgs production cross sections and Higgs branching ratios. Mixing of the Higgs doublet with a hidden sector captures modifications from the Standard Model Higgs phenomenology in the standard search channels in a representative way, in particular because invisible Higgs decay modes open up. As a consequence, LHC exclusion bounds, which disfavor a heavy Standard Model Higgs can be consistently understood in terms of a standard-hidden mixed Higgs system. Shedding light on the possible existence of such an admixture with a hidden sector and quantifying the resemblance of an eventually discovered scalar resonance with the Standard Model Higgs crucially depends on measurement of invisible decays. This task will already be tackled at LHC, but eventually requires the clean environment of a future linear collider to be ultimately completed.

1 Introduction

Recent measurements at the CERN Large Hadron Collider [1–4] constrain a SM-like Higgs to be lighter than $m_H \lesssim 130$ GeV at 95% confidence level. Moreover, both ATLAS and CMS have observed an excess for Higgs masses around 125 GeV, consistent with each other. These tantalizing hints for a light Higgs boson in the multilepton $H \to 4\ell$ and, more importantly, in the $H \to \gamma\gamma$ channels are in excellent agreement with theoretical expectations, which have been coined by electroweak precision measurements performed during the LEP era [5].

The accumulated statistics of approximately 5 fb^{-1} per experiment, however, is yet too small to draw a conclusive picture about mechanism of electroweak symmetry breaking. Since the assumption of SM-like production and decay explicitly enter the hypothesis tests that lead to the formulation of the LHC exclusion limits, the quantitative resemblance of the observed phenomenology with the SM is, in fact, not entirely transparent. Instead of mere numerical agreement of data with the SM Higgs hypothesis, we can understand the exclusion limits as a measure of how much a more general theory is bound to coincide with the SM in the light of current experimental observations. This exercise naturally yields model-dependent statements, but there is only a limited number of phenomenological patterns of how the Higgs can evade detection [6]. The extension of the Higgs sector by including invisible decay modes and constrain them by measurements is crucial for the re-interpretation of the exclusion bounds is this context. A substantial non-zero branching ratio would signalize a non-standard Higgs sector while being in perfect agreement with a non-observation of the Higgs at the moment.

Constraining invisible branching ratios is a difficult and challenging task at hadron colliders with their busy final states [7]. A statistically significant determination of an invisible Higgs branching ratio requires large statistics (if possible after all) as experimental systematics set the scale of uncertainty. Systematics vastly improves when studying the Higgs sector at a future linear collider. There, $e^+e^- \to HZ$ associated production provides an extremely clean laboratory process to study invisible decays in a model-independent way in recoil analyses [8]. At the LHC, only ratios of branching fractions are accessible in a model-independent fashion, but absolute branching ratio predictions can be formulated in specified models [9]. Hence, performing such an analysis at a future linear collider is going to be of utmost importance to study the Higgs boson in full detail after its discovery at the LHC.

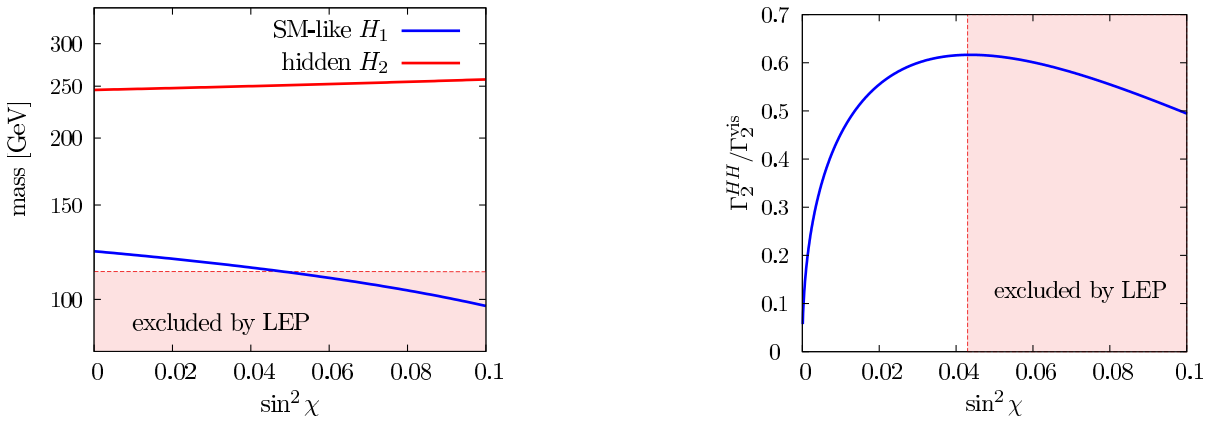

Figure 1: Left: masses of the light SM-like Higgs boson H_1 (blue) and the heavy Higgs boson H_2 (red). We choose the vacuum expectation values $v_h = v_s = 246$ GeV and $\lambda_s = \lambda_h/4 = 1/8$ for illustration purposes. The shaded region displays the LEP bound [5]. Right: cascade decay width Γ_2^{HH} as a function of $\sin^2\chi$ for the same parameters. Again, the region in which H_1 is excluded by LEP is shaded. The figures are taken from Ref. [10].

2 The Higgs portal

We introduce invisible decay channels in an efficient and theoretically consistent way via a particular type of hidden valley [11] interaction in the Higgs sector. The SM Higgs doublet ϕ_s is coupled to a hidden sector scalar field ϕ_h via the gauge-invariant and renormalizable operator $|\phi_s|^2|\phi_h|^2$ so that the potential reads [12]

$$\mathcal{V} = \mu_s^2|\phi_s|^2 + \lambda_s|\phi_s|^4 \;+\; \mu_h^2|\phi_h|^2 + \lambda_h|\phi_h|^4 \;+\; \eta_\chi|\phi_s|^2|\phi_h|^2\,. \tag{1}$$

The mass parameters μ_j can be substituted by v_j after expanding the two Higgs fields about their vacuum expectation values $v_j^2 = (-\mu_j^2 - \eta_\chi v_i^2/2)/\lambda_j$ $(i \neq j = s, h)$. The electroweak gauge boson masses are generated exclusively by the visible fields' vacuum expectation. The so-called Higgs portal interaction operator $\sim \eta$ rotates s, h states into the mass eigenstates

$$\begin{aligned} H_1 &= \cos\chi\, H_s + \sin\chi\, H_h \\ H_2 &= -\sin\chi\, H_s + \cos\chi\, H_h\,, \end{aligned} \tag{2}$$

where $\sin\chi$ is the characteristic mixing angle, which affects the production cross sections $\sigma_{1,2}$ and visible and invisible decay widths $\Gamma_{1,2}^{\rm vis,inv}$ of the two Higgs bosons in an universal fashion [9]

$$\sigma_{1,2} = \cos^2\chi\,\{\sin^2\chi\}\,\sigma_{1,2}^{\rm SM} \tag{3a}$$

and

$$\begin{aligned} \Gamma_1^{\rm vis} &= \cos^2\chi\,\Gamma_1^{\rm SM} \qquad \text{and} \qquad \Gamma_2^{\rm vis} = \sin^2\chi\,\Gamma_2^{\rm SM} \\ \Gamma_1^{\rm inv} &= \sin^2\chi\,\Gamma_1^{\rm hid} \qquad \text{and} \qquad \Gamma_2^{\rm inv} = \cos^2\chi\,\Gamma_2^{\rm hid}\,. \end{aligned} \tag{3b}$$

The index "SM" refers to the values in the SM, and the information on the hidden sector is encoded in the "hid" quantities. If kinematically allowed, *i.e.* for $m_{H_2} \gtrsim 2m_{H_1}$ we can have additional cascade decays (in the following we take H_1 to be the lighter, mostly SM-like state by definition), which, depending on the combinations of the fundamental parameters, can play a significant role [10]. We exemplarily show a Higgs spectrum as a function of $\sin^2\chi$ in Fig. 1. The relations between the suppression factors $\sin^2\chi$, the masses m_{H_1}, m_{H_2} and the fundamental lagrangian parameters of Eq. (1) can be obtained by straightforward calculation and we refer the reader to Refs. [9, 10] for further details.

The model of Eq. (1) is subject to constraints by electroweak precision observables and partial wave unitarity. A guiding principle toward the validity of a model is the comparison of the model's prediction of the Peskin-Takeuchi parameters [13] with measurements performed at LEP [5]. These give rise to the strongest constraints on the Higgs portal model*. This is easy to understand: for larger mixing angles $\sin^2\chi \to 1$ we effectively deal with a heavy Higgs model which is tightly constraint† by the measurements of [5]. At the same time, the isometry Eq. (2) restores unitarity in the high energy limit.

3 Higgs portal lessons from the LHC

Altogether the model predicts the four different phenomenological scenarios of Tab. 1 for standard Higgs resonance searches at typical LHC Higgs discovery luminosities ($\sqrt{s} = 14$ TeV), *cf.* Fig. 2, where we assume $\Gamma^{\rm hid} = \Gamma^{\rm SM}$ for simplicity. Apart from a small window in $\sin^2\chi$, the Higgs portal can be explored in its most symmetric version already at typical SM Higgs discovery luminosities [15].

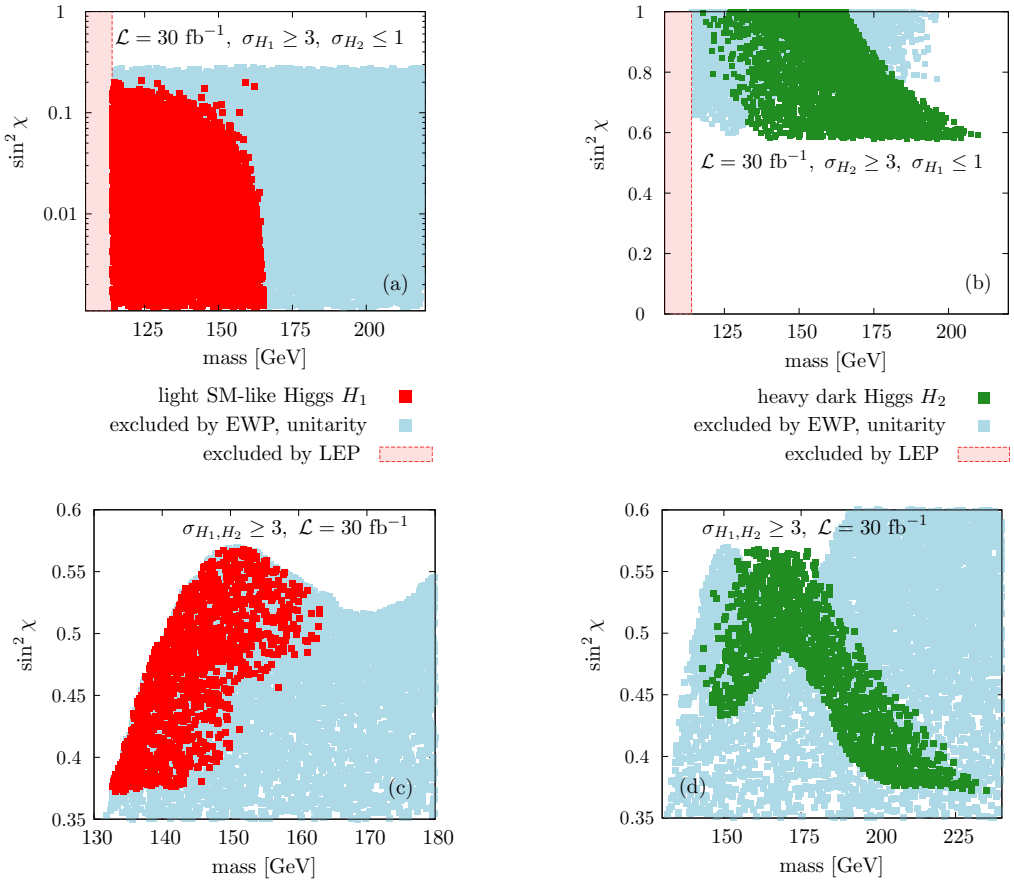

Figure 2: Scan over the Higgs portal model Eq. (1) for parameter ranges $v_h \in (0\text{ GeV}, 246\text{ GeV}], v_s = 246$ GeV, $\lambda_h \in (0, 4\pi]$, $\lambda_s \in (0, 4\pi]$, and $\eta_\chi \in [-4\pi, 4\pi]$. The hidden Higgs decay width is identified with the SM decay width for demonstration purposes, *i.e.* $\Gamma^{\rm hid} \equiv \Gamma^{\rm SM}$. LEP constraints and bounds from S, T, U [5] and unitarity are included. Panel (a) displays the sensitivity for H_1 only, panel (b) for H_2 only, and panels (c) and (d) show where the LHC is sensitive to both H_1 and H_2 at the same time for 30 fb^{-1} at $\sqrt{s} = 14$ TeV. The figures are taken from Ref. [10].

*For a discussion of perturbativity and stability of the potential Eq. (1) see Ref. [14].

†Note that in a realistic scenario we can expect kinetic mixing with a heavy $U(1)$ boson [14], which again loosens the electroweak precision constraints.

LHC sensitivity after 30 fb^{-1} to		
$\sin^2\chi \lesssim 0.2$	only H_1	$(\sigma_{H_1} \geq 3,\ \sigma_{H_2} \leq 1)$
$0.3 \lesssim \sin^2\chi \lesssim 0.4$	neither H_1 nor H_2	$(\sigma_{H_1,H_2} < 3)$
$0.4 \lesssim \sin^2\chi \lesssim 0.6$	both H_1 and H_2	$(\sigma_{H_1,H_2} \geq 3)$
$\sin^2\chi \gtrsim 0.6$	only H_2	$(\sigma_{H_1} \leq 1,\ \sigma_{H_2} \geq 3)$

Table 1: Result of Higgs searches at the LHC ($\sqrt{s} = 14$ TeV) with a luminosity of 30 fb^{-1}, σ refers to the sensitivity in terms of signal/$\sqrt{\text{background}}$.

Relaxing the assumption $\Gamma^{\rm hid} = \Gamma^{\rm SM}$ changes the picture. In fact, there is good reason to also consider the situation $\Gamma^{\rm hid} \gg \Gamma^{\rm SM}$, since the hidden decay width parametrizes our lack of knowledge about the dynamics in the hidden sector, which can be strong. To study the implications for general $\Gamma^{\rm hid}/\Gamma^{\rm SM}$ choices we examine the the 95% confidence level bounds which are formulated by the LHC collaborations with respect to the SM cross section. In the portal model of Eq. (1),(2) these can be expressed as [16]

$$\frac{\sigma[pp \to H_1 \to F]}{\sigma[pp \to H_1 \to F]^{\rm SM}} = \frac{\cos^2\chi}{1 + \tan^2\chi\,[\Gamma_1^{\rm hid}/\Gamma_{\rm tot,1}^{\rm SM}]} \leq \mathcal{R}\,, \tag{4}$$

where $\mathcal{R}$ denotes the observed exclusion limit. An identical quantity can be derived from future constraints on invisible decays [6, 7, 16]:

$$\frac{\sigma[pp \to H_1 \to inv]}{\sigma[pp \to H_1]^{\rm SM}} = \frac{\sin^2\chi\,[\Gamma_1^{\rm hid}/\Gamma_{\rm tot,1}^{\rm SM}]}{1 + \tan^2\chi\,[\Gamma_1^{\rm hid}/\Gamma_{\rm tot,1}^{\rm SM}]} \leq \mathcal{J}\,. \tag{5}$$

In Fig. 3 we exemplarily examine the implications of the current Higgs exclusion bounds for $m_H = 155$ GeV in the $\Gamma_1^{\rm hid}/\Gamma_1^{\rm SM}$-$\cos^2\chi$ plane. For this particular Higgs mass the experiments observe $R = 0.4$ [2–4]. From Fig. 3 we learn that there is a variety portal parameter choices which can accommodate the current phenomenological findings.

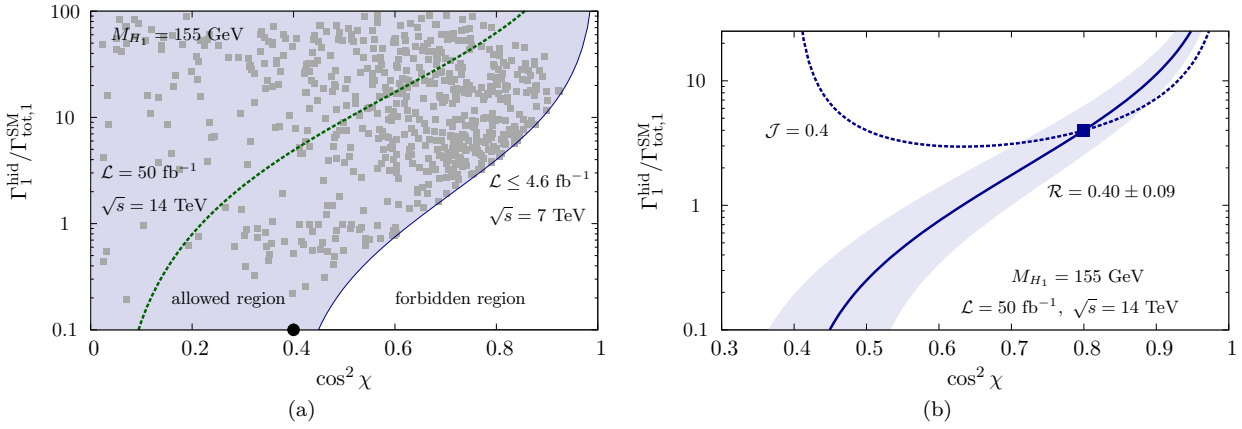

Figure 3: Left: bounds on the mixing and hidden decay width of H_1 for the point $M_{H_1} = 155$ GeV; $\mathcal{R} = 0.4$ in the standard-hidden Higgs scenario, based on current experimental results [2–4]. The regions dappled by small squares are compatible with unitarity and precision measurements. The dot indicates the $\Gamma_1^{\rm hid} \to 0$ limit of the exclusion curve at $\mathcal{R}$. The dotted line indicates the projected search limit for $\mathcal{L} = 50$ fb^{-1}. Right: bounds due to hidden Higgs searches at the LHC for established Higgs masses and cross sections. The figures are taken from Ref. [16].

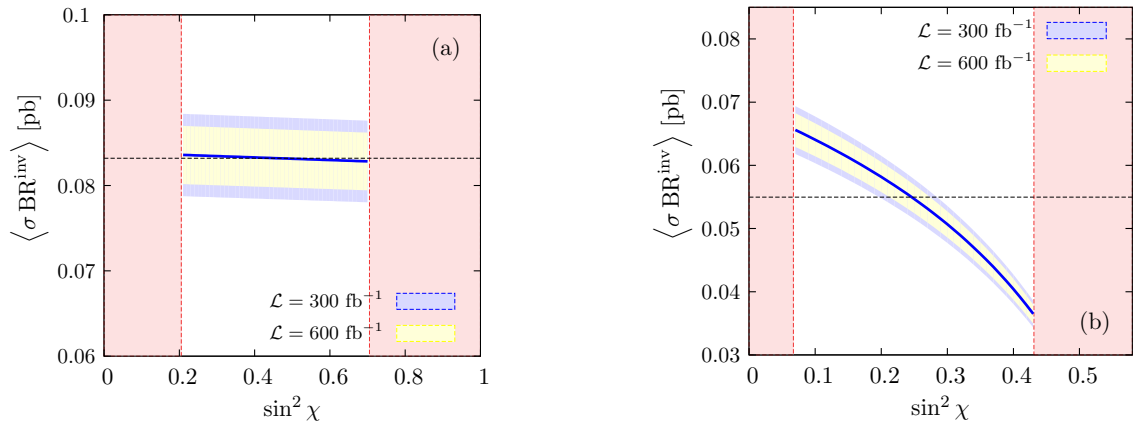

Figure 4: Reconstruction of the mixing angle from a measurement of the superposition of the invisible decays. The shaded area is theoretically not allowed due to positivity of the cross section ratio $\mathcal{R}_i$, uncertainties of these parameters are not considered. (a) is a degenerate mass spectrum $M_{H_1} = 140$ GeV, $M_{H_2} = 160$ GeV, (b) is a mass spectrum $M_{H_1} = 115$ GeV, $M_{H_2} = 300$ GeV, where the mixing can in principle be reconstructed due to Eq. (6) and comments below. Uncertainties follow from statistics only. The figures are taken from Ref. [10].

An additional constraint can be imposed in the same plane by constraining invisible decays at the LHC[‡]. Typically this involves large statistics when the [16] visible cross section of the H_1 state is already measured, *i.e.* the inequality of Eq. (4) becomes an equality within the uncertainty given by statistics and systematics. If $\mathcal{J}$ is yet to be understood as a 95% confidence level exclusion [7], we do not have the enough information to reconstruct the all parameters of Eq. (3).

In fact, when comparing to the SM Higgs potential, the multitude of observables which are potentially accessible in addition to the SM, *i.e.* the Higgs resonance masses and the cascade decay width if present, allow for a *full* reconstruction strategy of the Higgs portal potential Eq. (1). An absolutely crucial input for this analysis is the *measurement* of $\mathcal{J}$. The measurement of $\mathcal{R}$ for both Higgs states will eventually be possible at the LHC for the bulk of the parameter space. The measurement of $\mathcal{J}$ at the LHC, however, is limited by systematics [7] and the fact that we measure a superposition of invisible rates of the two Higgs states (on top of a challenging background) at hadron colliders

$$\langle \sigma \mathrm{BR}^{\mathrm{inv}} \rangle \sim f(\Lambda) - [\cos^2 \chi + \{\sigma_2^{\mathrm{SM}}/\sigma_1^{\mathrm{SM}}\} \sin^2 \chi] \,, \tag{6}$$

where $f(\Lambda)$ depends on the trilinear coupling (if accessible) in the invisible cascade decay $H_2 \to H_1 H_1 \to$ invisible. Even if a measurement turns out to possible, we rely on the separation of the two Higgs states to lift the degeneracy in the invisible decay channel (*cf.* Fig. 4). More concretely, in order to project out the $\cos^2 \chi$ component in Eq. (6) we need $\sigma_2^{\mathrm{SM}}/\sigma_1^{\mathrm{SM}} \ll 1$, *i.e.* $m_{H_2} \gg m_{H_1}$, unless we have a significant trilinear coupling in the resolved cascade decay, which can be used to constrain the mixing parameters.

In total the LHC can not cover the entire parameter space of the Higgs portal model Eq. (1).

4 Higgs Portal spectroscopy at a linear collider

The systematics-plagued determination of invisible branching ratio of the individual resonances can be cured at a linear collider. The clean LC environment allows a precise determination of the Higgs invisible branching ratio over a broad range of Higgs masses (see *e.g.* Ref. [8]). We exemplarily show the improvement due the measurement of $\mathcal{J}_1$ for the $m_{H_1} = 155$ GeV scenario discussed in Fig. 3b of the previous section in Fig. 5a.

[‡]Such an analysis has not been performed by the experiments, but exiting analyses were adopted in Ref. [6,17], demonstrating potentially sufficient sensitivity to $\mathcal{J} \sim 1$ for the combined 2011 data set.

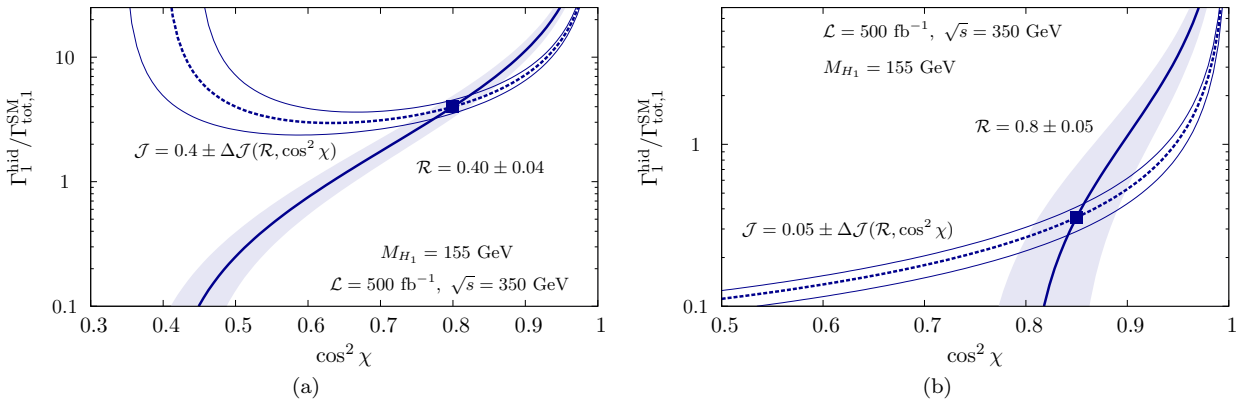

Figure 5: Left: the scenario of Fig 3b at a linear collider ($\sqrt{s} = 500$ GeV, $\mathcal{L} = 500$ fb^{-1}). Right: a Higgs portal scenario with small $\mathcal{J}$. The uncertainties are adopted from Refs. [8, 18], the figure are taken from Ref. [16].

From Fig. 5b it also becomes clear that the linear collider gives a good reconstruction of the Higgs portal for percent level values of $\mathcal{J}$.

Due to the measurement of both $\mathcal{J}_1$ and $\mathcal{R}_1$ we can reconstruct the intersection of both curves, yielding the mixing angle

$$\cos^2\chi = \mathcal{J}_1 + \mathcal{R}_1\,. \tag{7}$$

An independent measurement of $\sin^2\chi = \mathcal{J}_2 + \mathcal{R}_2$ overconstraints the system, giving rise to the sum rule

$$\mathcal{J}_1 + \mathcal{R}_1 + \mathcal{J}_2 + \mathcal{R}_2 = 1\,, \tag{8}$$

which can be used to test the consistency of the portal model Eq. (1) with experimental observations. We stress that this is not possible at the LHC due to Eq. (6).

Coming back to the strategy of approaching the SM with measurements that constrain $\Gamma_1^{\rm inv}/\Gamma_1^{\rm SM}$, it is worthwhile addressing the implications of the measured excess around 125 GeV for the portal model. If this

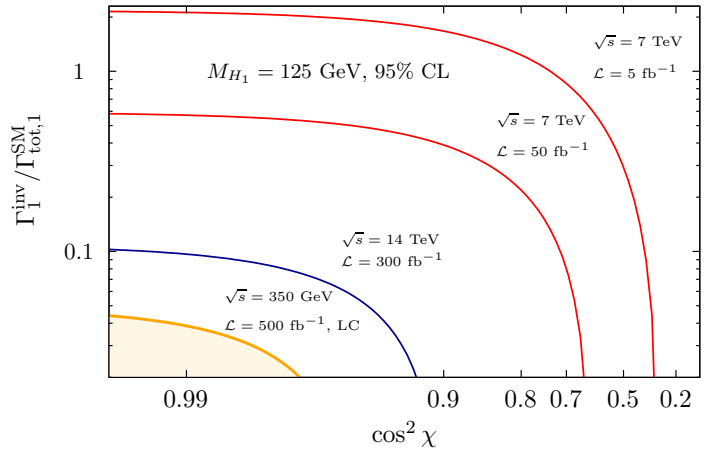

Figure 6: 95% CL contours for a measurement of $\Gamma_1^{\rm hid}/\Gamma_1^{\rm SM}$ at the LHC and a 350 GeV ILC. The LHC uncertainties are computed with SFITTER [19] and the LC uncertainties are again adopted from Refs. [18]; the figure is taken from Ref. [16].

turns out to be the Higgs then a measurement of $\Gamma_1^{\rm inv}/\Gamma_1^{\rm SM}$ give us a measure of the compatibility of the experimental observations with the SM.

Treating $\Gamma_1^{\rm hid}$ as a free parameter, we show 95 % confidence level contours in the $\Gamma_1^{\rm inv}/\Gamma_1^{\rm SM}$-$\cos^2\chi$ plane in Fig. 6. The blue and red lines correspond to measurements at the LHC, while the shaded are gives the prospects at a linear collider. Obviously the current findings at the LHC are not good enough from a statistical point of view to tell us wether or not we observe the SM Higgs. These bounds improve when higher center of mass energy and more integrated luminosity becomes available, but systematic uncertainties saturate the LHC sensitivity at around 300 fb^{-1}.

A future linear collider has the potential to take this LHC legacy to the next level: In Fig. 6 there is only a small region untested for the LC curve. For the chosen set-up of 350 GeV, 500 fb^{-1} the statistical and systematic uncertainties are comparable [8], hence further improvements can be expected by an even larger data sample.

Acknowledgments

References

[1] Atlas collaboration, ATLAS-CONF-2012-019. CMS collaboration, CMS-PAS-HIG-12-008.

[2] ATLAS Collaboration, G. Aad *et al.*, Eur. Phys. J. C **71**, 1728 (2011).

[3] CMS Collaboration, Phys. Lett. B**699** (2011) 25.

[4] ATLAS and CMS collaborations, ATLAS-CONF-2011-157, CMS PAS HIG-11-023.

[5] J. Alcaraz *et al.* [ALEPH Collaboration and DELPHI Collaboration and L3 Collaboration and], arXiv:hep-ex/0612034, [see also `http://lepewwg.web.cern.ch/LEPEWWG/plots/summer2006/`]. J. Erler and P. Langacker *in* K. Nakamura *et al.* [Particle Data Group], J. Phys. G **37** (2010) 075021.

[6] C. Englert, J. Jaeckel, E. Re and M. Spannowsky, Phys. Rev. D **85**, 035008 (2012).

[7] A. De Roeck, J. Ellis, C. Grojean, S. Heinemeyer, K. Jakobs, G. Weiglein, G. Azuelos and S. Dawson *et al.*, Eur. Phys. J. C **66** (2010) 525.

[8] M. Schumacher, LC-PHSM-2003-096.

[9] S. Bock, R. Lafaye, T. Plehn, M. Rauch, D. Zerwas and P. M. Zerwas, Phys. Lett. B **694** (2010) 44.

[10] C. Englert, T. Plehn, D. Zerwas and P. M. Zerwas, Phys. Lett. B **703**, 298 (2011).

[11] M. J. Strassler and K. M. Zurek, Phys. Lett. B **651**, 374 (2007). M. J. Strassler and K. M. Zurek, Phys. Lett. B **661**, 263 (2008).

[12] for early work see *e.g.* T. Binoth and J. J. van der Bij, Z. Phys. C **75**, 17 (1997). R. Schabinger and J. D. Wells, Phys. Rev. D **72**, 093007 (2005). B. Patt and F. Wilczek, arXiv:hep-ph/0605188.

[13] M. E. Peskin and T. Takeuchi, Phys. Rev. Lett. **65** (1990) 964.

[14] M. Bowen, Y. Cui and J. D. Wells, JHEP **0703**, 036 (2007) [hep-ph/0701035].

[15] Atlas collaboration CERN-LHCC-99-14, CERN-LHCC-99-15.

[16] C. Englert, T. Plehn, M. Rauch, D. Zerwas and P. M. Zerwas, Phys. Lett. B **707**, 512 (2012).

[17] O. J. P. Eboli and D. Zeppenfeld, Phys. Lett. B **495** (2000) 147

[18] J. A. Aguilar-Saavedra *et al.* [ECFA/DESY LC Physics Working Group Collaboration], hep-ph/0106315.

[19] R. Lafaye, T. Plehn, M. Rauch, D. Zerwas and M. Dührssen, JHEP **0908**, 009 (2009). M. Rauch, arXiv:1110.1196 [hep-ph].